Photoluminescence in hydrogenated amorphous silicon

D. J. Dunstan
Physics Department, University of Surrey, Guildford, Surrey GU2 5XH, England

F. Boulitrop
Laboratoire Central de Recherches, Thomson-C.S.F., Domaine de Corbeville, F-91401 Orsay Cédex, France

(Received 14 May 1984; revised manuscript received 26 June 1984)

By starting with exponential band tails of localized states, it is shown that the photoluminescence of *a*-Si:H can be explained with no further assumptions. The spectrum and its changes with temperature, with time, and with pump intensity and energy, and the decay curves and lifetime distributions, are predicted by the model, qualitatively, and, when the calculation is feasible, quantitatively.

I. INTRODUCTION

The luminescence of hydrogenated amorphous silicon has been extensively studied in recent years. Two principal emission bands are generally recognized, at about 0.9 and 1.4 eV (a review has been given by Street[1]). The low-energy band is thought to be due to defects, and is not our concern here. The high-energy band, which is the subject of this paper, is recognized to be due to the recombination of electrons and holes separately trapped in band tail states. Study of this emission may be expected to yield much information on the nature of the tail states; since these states dominate the electronic transport properties, a better understanding of them is of great technological as well of physical interest. Nevertheless, although Street *et al.*, in particular, have given a complete and comprehensive account of the photoluminescence (PL) mechanism,[1] there has been much controversy over most aspects of their model, and many authors have introduced further models to explain one or another detail of the experimental behavior of the PL.

In several recent papers, we have developed a new approach to the problem of the PL mechanism. We have proposed the simplest model consistent with the known physics of amorphous semiconductors: carriers are trapped at random, both spatially and energetically, in the tail states, and then undergo tunneling transitions, both radiative, to carriers in the other band, and thermalization (nonradiative) to lower tail states in the same band. We have found that, despite its simplicity, and indeed contrary to intuitive expectation, this model is nevertheless capable of predicting rather complex and apparently distinctive behavior which, in the literature, has often been explained by *ad hoc* additional models. The purpose of this paper is to collect together, and to discuss in more detail, the evidence and justification for our simple model.

The 1.4-eV PL band of *a*-Si:H is relatively featureless, compared with crystalline PL, and so yields little experimental information. Although it is the highest-energy PL band in *a*-Si:H, it is at a considerable depth below the optical gap ($E_{OG} \sim 1.9$ eV); the shape of the band is roughly Gaussian of width about 200–300 meV (Fig. 1). The decay of the emission intensity after pulsed excitation is nonexponential, being close to a power law, and therefore containing a wide range of lifetimes. These properties could be explained (since the material is amorphous) by suitable distributions of excited-state energies and radiative lifetimes. In fact, Street[2] attributes the width and position of the band largely to a Stokes shift, and most authors (see Ref. 1) account for the wide distribution of lifetimes in terms of separately trapped carriers, with a range of recombination distances.

Other experimental information comes from the dependence of the emission spectrum on excitation energy and intensity, and from time-resolved spectroscopy (TRS). Two breakpoints, or thresholds, have been identified: for excitation energies below about 1.8 eV the spectrum depends on the energy, and for excitation intensities above about 10^{18} cm^{-3} photocreated carriers per pulse, the decay curves in TRS change with excitation intensity. As discussed in Sec. II, these two breakpoints have induced a number of models.

A large body of experimental work on the PL is more concerned with nonradiative recombination. This includes the temperature quenching of the PL, studies of relative quantum efficiency in different samples and

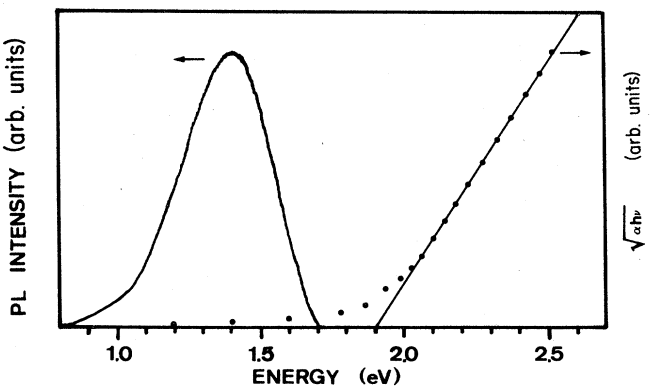

FIG. 1. Curve on the left is a typical 1.4-eV PL spectrum, and is compared with the absorption spectrum in the same sample (dotted curve) and the theoretical absorption spectrum of a parabolic band edge (straight line).

under different conditions, and much besides. Now, the nonradiative recombination (NRR) is not well understood; this may partly be due to the fact that it can only be studied indirectly, through the PL, and as long as the mechanism of the PL itself is not well established, interpretation of the NRR is uncertain. Consequently, this paper is restricted to the PL under conditions in which NRR is not dominant, that is, to PL in samples with a high quantum efficiency and at low temperature. We find, under this restriction, that a coherent and simple model can be developed; it may be hoped that extension to NRR will subsequently be possible.

Our model is based on the following considerations. From other experiments (optical absorption, electronic transport, etc.), there is considerable evidence that there is an exponential tail in the density of states, extending into the forbidden gap from the band edges. Indeed, the valence-band tail has recently been observed directly, by photoemission yield spectroscopy.[3] As far as possible, we account for the PL on the basis of the physics of these tails *only*. This approach is, in fact, remarkably successful, and it is primarily the internal coherence of the resulting model which enables us to question the justification of models which invoke Stokes shifts, thermalization gaps, geminate recombination, and other *ad hoc* mechanisms. That a model can be described as *ad hoc* is, of course, no criticism; it means only that the model is introduced specifically to explain the PL, and so that it should be dispensed with if possible.[4]

The organization of this paper is as follows. In Sec. II we review the evidence that has been put forward for other models of the PL mechanism; we describe these models and we give reasons for believing that they are not adequate or not necessary. Our model is presented in Sec. III; those aspects which we have described elsewhere will here be only very briefly mentioned. We show how it accounts for much of the experimental behavior of the PL: its spectrum and the spectral shifts under various perturbations, and the kinetics. In Sec. IV optically detected magnetic resonance (ODMR) results relevant to the model are discussed; and finally, in Sec. V we consider what information we can derive on the nature of the tail states and the electronic structure of *a*-Si:H, and, by extension, of amorphous semiconductors generally.

II. MODELS OF THE LUMINESCENCE MECHANISM

A. Kinetics

Although Engemann and Fischer[5] found a lifetime of 10 ns in the decay of the luminescence, and so proposed excitonic recombination, it soon became clear that the average lifetime is much longer than this, and that the decay is power law rather than exponential. Consequently, several groups proposed that electrons and holes are trapped separately, and that the recombination takes place through radiative tunneling transitions, as in donor-acceptor recombination in crystals.[6–8] The tunneling transition probability τ^{-1} depends exponentially on the pair separation:

$$\tau(r)=\tau_0\exp(\alpha r)\ , \tag{1}$$

where $2\alpha^{-1}$ is an effective Bohr radius; a distribution of electron-hole pair separations results in a wide distribution of radiative lifetimes and therefore in decay curves approximating to power laws. This interpretation has not subsequently been seriously questioned.

The trapping states themselves were variously identified as donors and acceptors,[6] and as the tail states of the Mott-Anderson model of disordered semiconductors.[2] This latter identification is now generally accepted, because the PL is observed in samples prepared in very different ways, and because it shows up to 100% quantum efficiency in any sample with a low density of states (less than about 10^{16}–10^{17} cm^{-3}). Jackson and Nemanich[9] deduce from photothermal deflection spectroscopy that the maximum efficiency in good samples is about 30%; this does not, however, affect the identification of the tail states as the radiative centers, for if the radiative states were defects or impurities, maximum quantum efficiencies $\sim 10^{-3}$ might be expected, at best, in proportion to the relative densities of tail states and other localized states.

Given that electrons and holes are separately trapped, the kinetics then depend on their relative spatial distributions. It is generally accepted that the tail states are distributed at random in space and energy, so that the distribution of available electron-hole separations is statistical. The simplest model is then that in which it is assumed that the carriers are indeed trapped wholly at random. Biegelsen *et al.*[10] and Tsang and Street,[7] however, proposed a correlation between the electrons and holes, due to a short diffusion length, so that a carrier would be trapped close to the carrier with which it was photocreated. These two carriers are referred to as a geminate pair. The evidence for this model came, firstly, from ODMR,[10] and secondly, from studies of the decay curve and its dependence on excitation intensity.[7] This interpretation of the ODMR data is not now generally accepted [see Ref. 62(b) and Sec. IV]. The geminate interpretation of the decay curves has been criticized by the present authors on both experimental[11] and theoretical[12] grounds (see also Ref. 52 and Sec. III D 2).

In the absence of geminate recombination, other phenomena such as thermal and electric field quenching of the PL are interpreted differently. In the geminate model, ionization of a geminate pair is taken to be a sufficient condition for NRR;[1] in our model it is not, and the NRR mechanisms need to be identified.

B. The spectrum

Much attention has been directed towards the PL spectrum, and its shifts under various perturbations (for a review, see Ref. 1). The excitation spectrum follows the intrinsic absorption edge with no evidence of an excitation band corresponding to luminescence centers;[2] nor is there any evidence of a higher-energy PL closer to the band gap (Fig. 1). Street[2] proposed that band-edge localized states have a considerable electron-phonon interaction (of some 200–250 meV), leading to a Stokes shift of 0.4–0.5 eV.

In this model, both the broadening of the intrinsic absorption edge (i.e., the exponential tail) and the depth and width of the PL emission band are due to this Stokes shift, and the zero-phonon energies of the radiative states are distributed over a relatively narrow band of energies at about 1.6 eV.

The evidence for the Stokes-shift model lies in its satisfactory fit to the experimental spectra, and also in a comparison between the absorption strength at the emission energies and the intensity of the emission at saturation (detailed balance). These points were discussed in Ref. 13, where we concluded that the case for a Stokes shift was not proven; in this paper we therefore assume that the tail states are rigid, in order to keep the number of free parameters to a minimum.

The spectrum shifts, both absolutely and relative to the band gap, under suitable conditions. It shifts to lower energy at elevated temperature, under reduced excitation energy, and at long decay times in TRS. There is a weak blue shift with excitation intensity; Bhat *et al.*[14] also report an anomalous blue shift when the excitation energy is reduced at high temperature. The shift with time has been attributed to a correlation between depth in the tail and localization; however, in order to account for it in detail, it has been found necessary to introduce a Coulomb shift[15] and carrier diffusion.[16] Continuing thermalization during the decay has also been proposed;[15] this explanation is generally accepted at least for times of the order of nanoseconds.[17] It is also the explanation which emerges from our model (Sec. III C 3).

The red shift with temperature is greater than that of the gap; it is understood qualitatively in terms of thermal excitation to the bands of the shallower states of a distribution. It has also been suggested that it may be due to faster thermalization at higher temperature. The blue shift with excitation intensity is thought to be due to saturation of the deeper states.

The red shift with excitation energy has attracted the most attention. Chen *et al.*[18] have suggested that it implies the existence of a thermalization gap; in this model the photoexcited carriers are trapped first in shallow tail states and then thermalize down through the tail. At some energy, the density of tail states is sufficiently low that further thermalization becomes unlikely compared with radiative recombination; this energy is the thermalization gap. When the excitation energy is reduced below the band gap, direct excitation into the deeper tail states below the thermalization gap becomes relatively more important, and the emission shifts to the red. The thermalization gap is found to be 1.6 eV; a Stokes shift is then invoked in order to obtain the observed PL spectrum.[18] Our analysis of thermalization in an exponential density of states does not predict a thermalization gap and yet yields the observed red shift;[13] the concept of a thermalization gap is therefore unnecessary.

Many authors have explained the PL spectrum without recourse to a Stokes shift, by assuming a density of radiative states corresponding to the emission spectrum (see, e.g., Refs. 19–21, and references therein). This is an assumption that we do not find necessary to make: the exponential tails alone account for the emission spectrum.[22]

C. Nonradiative recombination (NRR)

The primary effect of NRR on the emission band is, of course, a reduction in its efficiency. Further effects are possible on, for example, the decay curve, or the temperature quenching curve; these effects depend on the NRR mechanism.

Three mechanisms of NRR have been identified by Street.[1] At low temperature and low excitation pump rate, the dominant NRR occurs through tunneling to defects (identified, by comparison with ESR, as dangling bonds). The dependence of the quantum efficiency on defect density is in reasonable agreement with this model[23,24] (but see also Refs. 25 and 26). At high excitation rates, the PL intensity becomes sublinear against excitation; Street[27] has proposed that this is due to Auger recombination when the geminate pairs overlap. Finally, thermal ionization of geminate pairs allows diffusion and subsequent NRR at defects.[1]

The dependence of the PL intensity on defect density, on the intensity of the excitation, and on temperature is complicated. Nevertheless, it has been successfully accounted for in terms of these three mechanisms.[1] However, recent results that were not predicted by this model show that the NRR is not yet understood. Collins *et al.*[25] found that the decay curves in TRS are remarkably similar in samples with very different defect concentrations; they suggested that in their samples direct capture into defects was dominant over tunneling. Bhat *et al.*[14,28] showed that excitation below the gap changes the kinetics completely, so that the PL intensity—at low excitation rates—is no longer linear with pump rate. Finally, Wake and Amer[29] observed that carrier lifetimes measured by photoabsorption at high temperature are longer in the presence of a high density of dangling bonds.

These recent results are not yet understood; consequently, we do not take results involving NRR into account either in formulating or in testing our model.

D. Justification for a new model of the PL

The principal problem with the models described above, in Secs. II A and II B, is simply that there are too many of them. The PL of *a*-Si:H is featureless, compared with a typical crystal emission—that is, it carries much less information. It is therefore possible for many models to fit the data; our criticism is thus not that these models do not fit the PL, but that they do not explain it. All these models have two fundamental features in common: they all accept that there is some distribution of zero-phonon energies, and they all assume that the electrons and holes are separately trapped. It is undesirable to introduce further assumptions if these two alone can explain the data.[4]

Of secondary importance is the fact that there are some difficulties, experimental or theoretical, for some of the details in these different models. Thus, frequency-resolved lifetime measurements show that even at low excitation intensity recombination is not geminate, but distant pair,[11] and even the assumptions of the geminate model can be shown to result in distant-pair recombination.[30] Similarly, analysis of thermalization in an ex-

ponential density of states does not predict a thermalization gap. A Stokes shift, which gives a Gaussian emission spectrum, would also be expected to give a Gaussian edge on the excitation spectrum, rather than the exponential edge that is observed. There is strong evidence that thermal diffusion of the electrons dominates the kinetics even at temperatures as low as 80 K;[31,32] at this temperature thermal quenching of the PL is negligible. It follows that ionization of geminate pairs cannot be the rate-limiting step in NRR.

We conclude that there is good reason to analyze the PL using only the two assumptions above: that there is an exponential distribution of excited-state energies, and that the carriers are trapped separately at random. Other information will be used only when it is solidly founded on experiment (preferably other than PL). And, in the next section we shall see that this is, indeed, sufficient to account for the 1.4-eV PL of *a*-Si:H.

III. DERIVATION OF THE LUMINESCENCE FROM THE BAND TAILS

A. The band structure

According to the Anderson-Mott picture of amorphous materials, a mobility edge separates the band, of delocalized states, from a tail of localized states.[33] This tail is observed directly in photoemission yield spectroscopy[3] and is accurately exponential from the valence-band edge over up to several decades of density of states. There is evidence, from transport measurements[34,35] and from ESR,[36] that in *a*-Si:H the valence-band tail is about 3 times deeper than the conduction-band tail. Redfield[37] showed that in this case the deeper tail dominates the absorption spectrum; we may therefore identify the exponential absorption tail with the valence-band tail. This is consistent with the slopes observed in absorption and in photoemission yield spectroscopy. Assuming that the conduction-band tail is also exponential, we write

$$N_i(\epsilon)=N_{0i}\exp(-\beta_i\epsilon), \quad i=c,v \tag{2}$$

for the densities of states of the tails, where ϵ is the depth from the band edge i, and N_{0i} are the densities of states at the mobility edges. (There is no particular reason to assume that N_{0i} should have the same value for the two bands, but the exact values are not important in our model.) The slopes β_i will be given by $\beta_v \sim 16$ eV^{-1} (from the absorption spectrum, and consistent with the values observed by Griep *et al.*[3]) and $\beta_c \sim 50$ eV^{-1}. It is generally assumed that the tail states are neutral when empty; they trap carriers by a short-range potential. However, at sufficient distance from the center, the wave functions may be expected to decay exponentially, and we may use Eq. (1) for tunneling transitions. The parameter α is related to the Bohr radius or characteristic length r_0 of the exponential decay of the larger wave function by $\alpha=2/r_0$.

The parameters α and τ_0 in Eq. (1) are not known from other data; from their analysis of PL quenching by dangling bonds, Street *et al.*[24] deduced that the Bohr radius of the wave function of the conduction-band tail states is 12 Å. For the radiative recombination transitions, they used a prefactor τ_{0r}^{-1} of 100 MHz and for nonradiative transitions $\omega_0=\tau_{0nr}^{-1}=1$ THz. These values might be somewhat model dependent (see Sec. III C 1); however, on theoretical grounds they are not unreasonable. For an allowed direct optical tunneling transition, Hoogenstraaten[38] gave an analysis in which he showed that the prefactor is the same as the transition rate of band-to-band (delocalized) transitions.

Our model is shown schematically in Fig. 2. Radiative transitions are allowed between occupied tail states of opposite sign, and nonradiative tunneling transitions are allowed to lower unoccupied tail states of the same sign, and to defects. All transition rates are given by Eq. (1) with the parameter values given by Tsang and Street.[7] Photoexcited carriers are trapped in the tail states, in a short time compared with the tunneling transitions. This assumption is consistent with photoconductivity measurements at low temperature.[39] There is no direct evidence that the capture cross section of a tail state depends significantly on its depth; we therefore assume that the initial distribution of trapped carriers follows the density of states [this assumption is also used in the multiple trapping model (MTM) of dispersive transport: see, for example, Ref. 40]. In contrast to the MTM, we need to take into account transitions among the tail states (i.e., hopping). At low temperature these are downwards only; thermally induced upwards transitions will be important to the temperature dependence of the PL.

We shall first show qualitatively how these assumptions lead to a successful prediction of the experimental behavior of the PL; in Sec. III C we submit the model to a more quantitative and rigorous analysis.

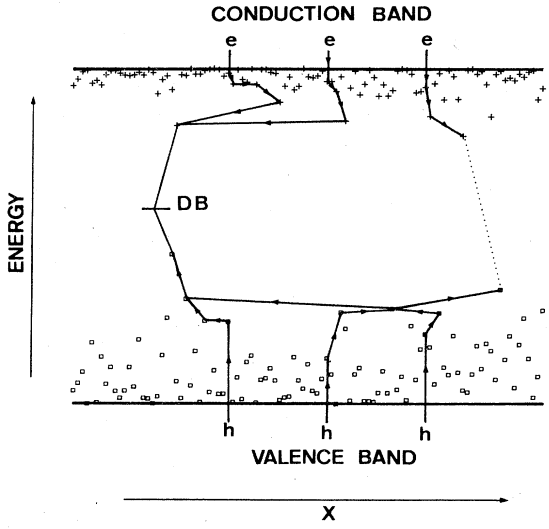

FIG. 2. One-dimensional representation of the model used to describe the PL. The tail states are indicated by the pluses [conduction band (CB)] and squares [valence band (VB)]; their depths are exaggerated by a factor of 3 for clarity. Three electron-hole pairs have been introduced; thermalization transitions are shown by solid lines and radiative transitions by dotted. Two pairs recombine on a defect (DB). This diagram was generated by a Monte Carlo program, using $\rho=1$, $\alpha^{-1}=5$, and $\tau_0\omega_0=10^4$.

B. Qualitative behavior of the model

Photoexcited carriers will thermalize rapidly to the band edges and diffuse some distance apart which will depend on the excitation energy. This initial separation will be ignored. Once trapped in the tail states, the carriers will make nonradiative transitions among the tail states, to lower energy, until they undergo radiative (or nonradiative) recombination. At each thermalization transition, the distribution of distances over which a thermalization transition is possible depends on the density of lower tail states. In contrast, because of the exponential form of the tails, the distribution of energies lost in a thermalization transition is constant. It is clear that the carriers will descend very quickly through the upper part of the tail: at tail-state densities of 10^{20} cm^{-3} the transition times will be subnanosecond. It is for this reason that the absolute densities of tail states, $\beta_i^{-1}N_{0i}$, are of little importance. The interesting part is lower down, where the thermalization transition rates become comparable to the radiative tunneling rates; that is, roughly, where the density of tail states becomes comparable to the density of carriers. A change of a factor of e thus has only the effect of shifting the interesting part up or down by the energy $1/\beta$: it shifts the entire spectrum but does not change its form or kinetics.

The spatial position of the carrier relative to the point where it was first trapped is determined by a random walk in which the steps have a distribution of values; for each successive step, this distribution shifts to larger values. The radiative lifetime also has a distribution of values, depending on the density of carriers of the other sign. For typical experimental conditions, the average radiative lifetime is about 1 ms.[7,11] The final thermalization transitions will be over distances corresponding to this time, which, for the parameter values given above for electrons, are about 125 Å. Neglecting the Coulomb interaction between electron and hole, it is then quite unlikely that a geminate pair will remain within a few tens of angstroms (as required by the geminate model[1]). Instead, the carriers of the pair are expected to move apart further than a reasonable distance for a subsequent optical transition; they can be treated as if they have lost all spatial correlation and are trapped at random.[12,41] We return to the subject of the Coulomb interaction below.

The transition rate among the tail states does not depend on the initial and final energies, except insofar as the initial energy is correlated with the distribution of distances to lower tail states. Consequently, the chance that a tail state receives a carrier thermalizing from above is independent of its energy (the probability is determined by the local configuration of other tail states, both above it and below it). On the other hand, each tail state has a very different probability of losing a carrier to lower states; this probability is determined by the local arrangement of lower states and is strongly correlated to the energy of the state. The probability of radiative recombination depends on the local arrangement of carriers in the other band in the vicinity. It is easy to see that, for sufficiently deep tail states, the branching ratio in favor of radiative recombination approaches unity, while for sufficiently shallow states, it vanishes. The details of how the branching ratio goes between these values will be discussed in the next section; here it is sufficient to note that it will not be a sharp transition, for the quantities that determine the tunneling probabilities have a wide range of values at any given tail-state energy.

It is important to note that there is no thermalization edge—that is, no energy below which the occupation probability decreases, after thermalization is complete. The occupation probability is constant down the entire tail after the carriers are first trapped, and thereafter increases monotonically with depth in the tail. A thermalization gap would arise only if carriers were necessarily trapped in shallow states before thermalizing to deeper states; this corresponds to the possibility of a higher occupation probability high in the tail at some stage of the thermalization. It is not clear what physical property could give rise to this behavior, other than a much larger capture cross section for shallower tail states, and for this there is no evidence.

The PL spectrum is given by the probabilities of occupation and of radiative recombination from a state as a function of its energy below the band edge, and convolved over the two bands. We have given simplified calculations elsewhere,[13,22] which fit the experimental spectra reasonably well (see Sec. III C). The shifts of the spectrum with temperature and with excitation energy are obtained by applying suitable weighting functions to the occupation probabilities. This has been analyzed in detail in Ref. 13 and will not be repeated here.

The blue shift with excitation power is due to two effects. Firstly, the lower tail states, which have anyway a high occupation probability, become saturated. Secondly, as the density of carriers is increased, the radiative lifetimes become shorter and the branching ratios for radiative recombination increase all the way up the tail, therefore shifting the emission band to higher energy.

The red shift observed with decay time in TRS is here explained without recourse to any correlation between depth and localization length. Measurement of the spectrum at short times corresponds to measurement after fewer thermalization transitions; consequently, the emission is at higher energy.

The exact mechanism of nonradiative recombination is not clear; however, on the assumption that it is due to competitive tunneling to defects,[7] then in this model the defects need only be included in the distribution of states as the lowest states to which thermalization transitions can take place. Possibly, a different capture cross section might be required; there is, however, no direct evidence for this.[42]

At low temperature, the kinetics are determined by tunneling. There are two interesting consequences that we wish to draw attention to. If it is assumed that complete thermalization precedes any radiative recombination, then an analysis of the kinetics in terms of distant-pair recombination without diffusion will be applicable.[12,26] During the decay, the close electron-hole nearest-available-neighbor pairs recombine first, leaving a distribution of pairs with larger separations. Because the lifetime increases exponentially with separation, there remains final-

ly a metastable density of electron-hole pairs whose radiative lifetimes exceed any reasonable experimental lifetime—in a-Si:H this density is some 10^{17} cm^{-3}. This metastable population is of profound importance in measurements of the kinetics, for it provides an upper limit to the possible lifetimes of carriers inserted into it. This is sufficient to explain the transition from first- to second-order kinetics observed at pulse intensities of about 10^{18} cm^{-3}.[12] However, in the model as discussed here, the nonradiative transitions are faster than the radiative transitions for a given separation, by a factor of about 10^4.[7] The kinetics are then dominated, not by the radiative transitions, but by the thermalization transitions. This point is discussed in Sec. III C, and could lead to a revision of the parameter values used in Eq. (1) to fit a-Si:H.

Finally, we consider the question of the Coulomb interaction between electrons and holes and its effect on the statistics of the thermalization transitions. The strength of the Coulomb interaction is not known; Street[15] used $\epsilon=12$ in

$$E_c(r)=e^2/(4\pi\epsilon\epsilon_0 r) \tag{3}$$

and showed that this was consistent with the time-resolved peak energy of the spectrum.

The Onsager formalism[43] may be applied to the diffusion of a pair of charged carriers under the influence of the Coulomb interaction, and Noolandi *et al.*[44] treated diffusion in a-Si:H in this way. Starting from the experimentally determined decay curve at low temperature, they were able to derive the decay curve at high temperature. However, we have seen above that the thermalization transitions are between states whose energies are different by amounts which are not small compared with the Coulomb energy; and larger still when compared with the change in Coulomb energy in a transition. The Coulomb interaction may be expected to have much less effect on the final spatial distribution than in the case treated by Onsager[43] (electrolyte dissociation in solution), where the Coulomb energy is the only difference between the initial and final energies of each step in the random walk. Furthermore, the steps in our random walk are over distances sufficiently large (up to and exceeding 100 Å) that random electric fields in the material (as proposed by, e.g., Fritzsche[45] and Tauc[46]) will have effects at least comparable with the effect of the Coulomb interaction between carriers. Finally, Merk *et al.*[32] were able to derive the high-temperature PL decay curves without reference to low-temperature data, by applying the MTM model without including any effect of a Coulomb potential on diffusion. In these circumstances, we believe that it is reasonable to omit the Coulomb interaction from the model.

C. Quantitative analysis of the model

A complete and rigorous analysis of the model does not appear to be feasible: there are too many parameters with randomly distributed values. It is possible that a Monte Carlo approach would be of value. Here, we shall give a number of approximate solutions, which, we hope, will display the essential features of the model. We begin with some discussion of the values of the parameters that appear in the calculations.

1. Parameter values

Photoemission yield spectroscopy gives a reliable estimate of the density of states of the valence-band tail, $N_{0v}\sim 1\times 10^{21}$ cm^{-3}eV^{-1}, and 16 eV^{-1} may be taken as an average value for β_v since it can vary from $\sim$12 to 20 eV^{-1} according to sample preparation.[3] Unfortunately, the same technique cannot be used for the characterization of the conduction-band tail, possibly because the optical transition to higher states in the conduction band may be forbidden [S. Griep (private communication)]. The tail of the optical-absorption spectrum is dominated by the valence-band tail and thus cannot give any information about the conduction-band tail,[37] but does confirm the results of photoemission yield spectroscopy for the valence-band tail. From ESR measurements in n-doped samples and their correlation with dark conductivity activation energies, β_c has been estimated to be about 30 eV^{-1}.[36] This value seems a little low compared with the 40—50 eV^{-1} from thermally stimulated current (TSC) measurements,[35] and with other transport measurements from which the conduction-band tail is estimated to be 2 to 3 times shallower than the valence-band tail.[34] Our measurements of activation energies[31] also suggest a factor of 3. We take $\beta_c=40$ eV^{-1}. The total density of tail states in each band would not be expected to be very different; for simplicity we take them to be equal and so we write $N_{0c}=N_{0v}\beta_c/\beta_v$.

Parameter values for the kinetics are more difficult to establish. The preexponential factor τ_0^{-1} for the radiative tunneling rate has not been directly measured, but is expected to be similar to the values observed in other direct gap semiconductors, some 10^8—10^9 Hz. The former value is generally used for a-Si:H;[7] since none of the experimental interpretation is particularly sensitive to this parameter, we use the same value. The nonradiative tunneling preexponential for the thermalization rate among tail states, ω_0, is expected to have the value of a typical acoustic-phonon frequency; again, this value has not been measured. We follow Tsang and Street[7] who used the value of 10^{12} Hz.

From the geminate-bimolecular transition at 10^{18} cm^{-3}, a Bohr radius r_0 of 12 Å was deduced[7] for the wave function of the less strongly localized band tail states (the conduction band). The interpretation of the transition is questioned,[11] but the same value can be estimated from the correlation between the PL quantum efficiency and the density of nonradiative centers measured by ESR.[24] A smaller value, $r_{0v}=6$ Å, may be taken for the deeper and presumably more strongly localized valence-band tail states. All the parameter values we use are summarized in Table I.

2. The spectrum

We begin by calculating the spectrum using the method of Ref. 13. By taking a single radiative lifetime (of 1 ms), thermalization transitions can occur up to this time; this corresponds to transitions among the conduction-band

TABLE I. Parameter values for valence- and conduction-band tails. $E_{0g}=2$ eV at 5 K for the sputtered sample, and 1.85 eV at 5 K for the glow discharge sample of Ref. 6; $\tau_0=10^{-8}$ s; $\omega_0=10^{12}$ Hz.

	N_i ($cm^{-3}eV^{-1}$)	β_i (eV^{-1})	r_{0i} (Å)
Valence-band tail	10^{21}	16	6
Conduction-band tail	3×10^{21}	40	12

tails over distances up to 125 Å for the parameter values of Table I. The radiative transitions then occur from tail states that are the lowest tail states within spheres of radius $r_c=125$ Å; setting V for the volume of these spheres and

$$\rho_i(\epsilon)=N_{0i}\beta_i^{-1}\exp(-\beta_i\epsilon)$$

for the density of tail states at energies lower than ϵ, we obtain for the probability that a given tail state at energy ϵ is the deepest within V,

$$P_{Li}(\epsilon)=\exp[-V\rho_i(\epsilon)]\ . \tag{4}$$

Then the density of tail states that are the deepest states within volumes V is given by

$$\begin{aligned}P_i(\epsilon)&=N_{0i}\exp(-\beta_i\epsilon)\exp[-V\rho_i(\epsilon)]\\&=N_{0i}\exp(-\beta_i\epsilon)\\&\quad\times\exp[-\tfrac{4}{3}\pi r_c^3N_{0i}\beta_i^{-1}\exp(-\beta_i\epsilon)]\ .\end{aligned} \tag{5}$$

These densities are plotted in Fig. 3 (dashed curves). The PL spectrum is then obtained by a convolution of the two densities for the conduction and valence bands. This is shown and compared with two experimental spectra in Fig. 4. One spectrum is taken from sputtered a-Si:H (curve a); the other is from a glow discharge sample from Street *et al.* (curve b) and has been replotted from Street and Biegelsen.[47] The theoretical curve (c) shows good agreement with the experimental spectra for both the energy and the asymmetry of the shape of the spectrum. However, the theoretical spectrum is narrower than the experimental spectra, especially for the sputtered sample. A more rigorous calculation requires that we take into account the occupation probabilities of the tail states while considering the thermalization transitions; since these vary with time, such a calculation is more appropriately carried out in connection with time-resolved spectra. The calculation is given in the next section; the result for the spectrum under continuous excitation is shown in Fig. 4 (curve d). Agreement with the experimental curves is improved as far as the width is concerned, while remaining excellent for the shape and position of the spectrum.

3. *Red shift with decay time*

Time-resolved spectra are recorded through a gate at fixed delay times after an excitation pulse. If the lifetime distribution is sufficiently flat (see Sec. III D) and the delay between pulses sufficiently long (see Ref. 48), then the emission observed at a delay time τ_d comes from centers with a decay time τ_r close to τ_d according to

$$I(\tau_d,\tau_r,t)=\tau_r^{-1}\exp(-t/\tau_d)P(\tau_r)\ .$$

The approximation of Eq. (5) is particularly well suited to calculating these spectra, since putting the delay time τ_d for the radiative lifetime τ_r is all that is necessary. Indeed, the calculation should be more exact than its application in Sec. III C 2. However, to calculate the spectrum more rigorously than in Sec. III C 2, the occupation

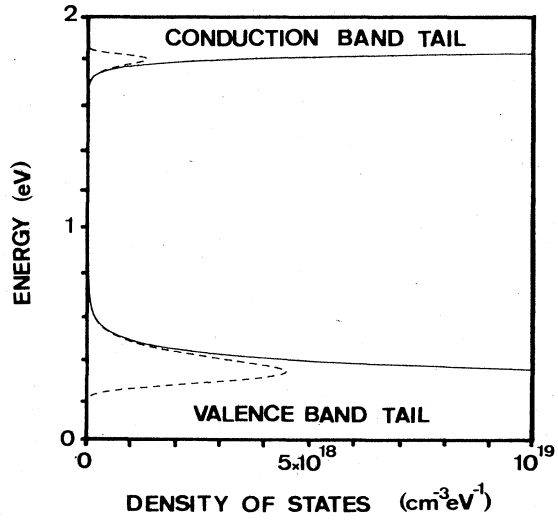

FIG. 3. Density of states of the band tails are shown together with the density of local minima after 10 ms of thermalization.

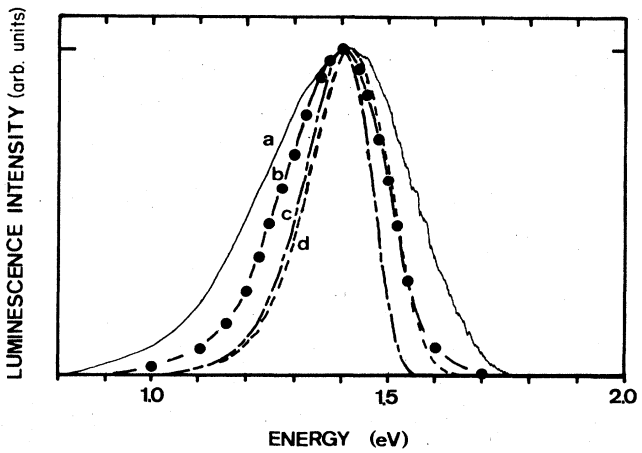

FIG. 4. Two experimental PL spectra are shown, for sputtered a-Si:H (curve a) and glow discharge (curve b, taken from Ref. 47). The theoretical spectra are calculated from Eq. (5) with use of a radiative lifetime of 10 ms (curve c) and Eq. (6) with use of an experimental lifetime distribution (curve d).

probabilities of the lower tail states must be included; the calculation is done in terms of the evolution with time of the system. The density of photoexcited carriers in tail i, at a depth ϵ below the band edge, at time t after a short excitation pulse, is given by

$$D_i(\epsilon,t)=Q(t)N^{-1}\exp(-\beta_i\epsilon)\exp[-V(t)\rho_i(\epsilon,t)] \quad (6)$$

with

$$N=\int_0^\infty \exp(-\beta_i\epsilon)\exp[-V(t)\rho_i(\epsilon,t)]d\epsilon$$

and $Q(t)$ is the density of photoexcited carriers which have not recombined at time t, given by

$$Q(t)=Q_0\int_0^\infty P(\tau)\exp(-t/\tau)d\tau$$

where Q_0 is the density of photoexcited carriers at $t=0$ and $P(\tau)$ is the lifetime distribution,

$$V(t)=\tfrac{4}{3}\pi[\alpha^{-1}\ln(t\omega_0)]^3 , \quad (7)$$

$$\rho_i(\epsilon,t)=N_{0i}\beta_i^{-1}\exp(-\beta_i\epsilon)-\int_\epsilon^\infty D_i(u,t)du .$$

The last quantity is the density of unoccupied tail states below the energy ϵ at time t.

These equations are solved numerically starting from $t=0$, yielding the results shown in Fig. 5. The PL spectrum is obtained by convolution of both distributions and using the experimental lifetime distribution for $P(\tau)$ (Sec. III D 5), and is shown in Fig. 4 (curve d). The shift with delay time of the luminescence peak energy at low temperature, including the Coulomb correction term E_c is shown in Fig. 6(b) together with experimental data measured in a sputtered a-Si:H sample for comparison. Some data taken from Tsang and Street[7] for glow discharge a-Si:H is also shown. Note that the good agreement with the data is achieved without any fitting parameters.

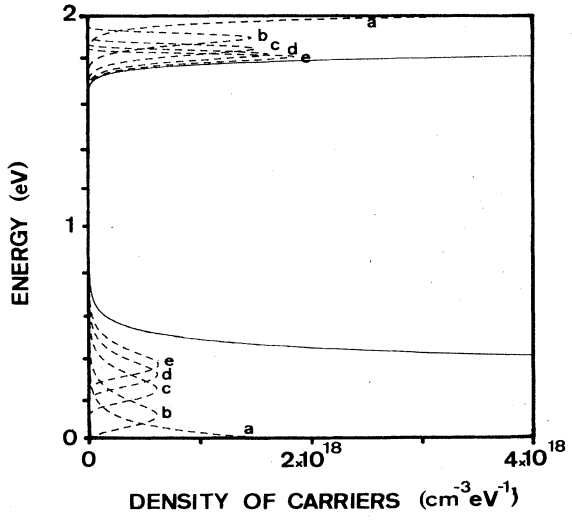

FIG. 5. Density of occupied tail states during thermalization is shown as a function of time, calculated from Eqs. (6) and (7) and assuming that there is no recombination. Curve a: 10^{-12} s, curve b: 10^{-9} s, curve c: 10^{-6} s, curve d: 10^{-3} s, and curve e: 1 s.

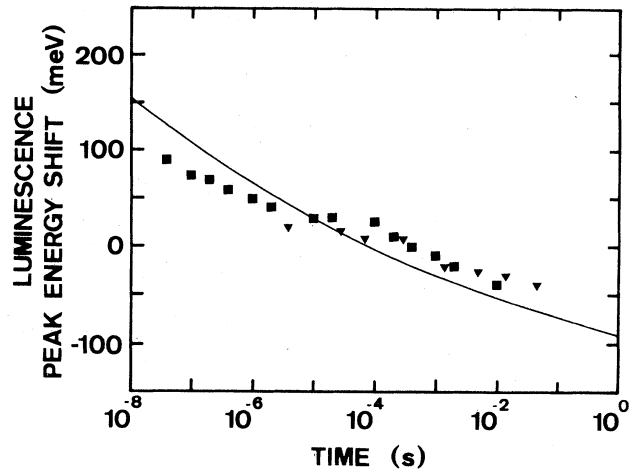

FIG. 6. Experimental shift of the peak energy of the luminescence with decay time in TRS in sputtered a-Si:H at 5 K (triangles) and (taken from Ref. 7) glow discharge (squares) at 12 K. The solid curve is obtained from the calculation of Eqs. (6) and (7).

4. *Blue shift with excitation intensity*

As the excitation intensity, or pump rate, increases, the lifetime distribution shifts towards shorter times,[7,11] as discussed below in Sec. III D 5. Since the lifetime distribution appears in the theoretical calculation of the spectrum, its evolution with the excitation intensity should yield the evolution of the spectrum. Setting the lifetime distributions of Sec. III D 5 into the calculation of the preceding section, we obtain the theoretical spectra shown in Fig. 7(a). Agreement with the experimental spectra [Fig. 7(b)] is good.

5. *Red shifts with temperature and excitation energy*

These calculations were previously reported[13] and will not be repeated here. Good agreement with experiment

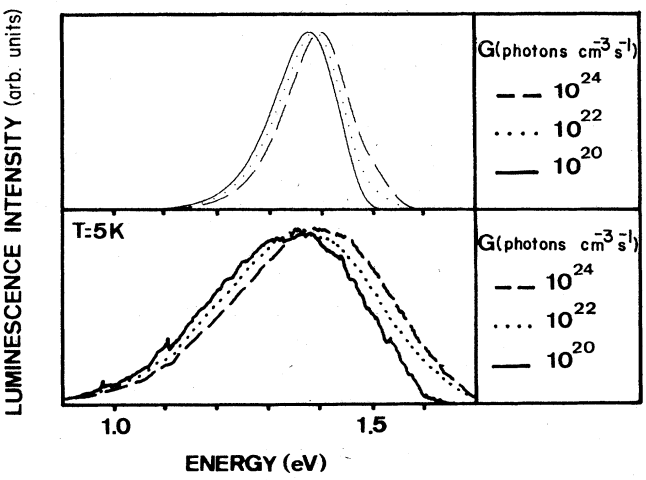

FIG. 7. PL spectra taken in sputtered a-Si:H at different excitation intensities. Theoretical spectra are computed from Eq. (6) using the experimental lifetime distributions shown in Fig. 8.

was found, simply by weighting the contribution of the minima at different depths in Eq. (5) by appropriate factors.

6. An anomalous blue shift

Bhat *et al.* recently reported a blue shift as the excitation energy is reduced, at temperatures above about 150 K.[14] This shift is anomalous, in that it is the opposite to the shift observed with excitation energy at low temperature (Sec. III C 5), and unexpected. No explanation has yet been proposed; Bhat *et al.* indeed suggested that it could only be due to a second, separate, PL mechanism under low-energy excitation. However, here we demonstrate that this blue shift is, at least, not inconsistent with the model of the photoluminescence used throughout this paper.

At temperatures as high as 150 K, the luminescence is severely affected by the temperature. Its peak energy is shifted considerably to the red, by $\sim$100–200 meV; this effect is understood.[13] The kinetics are profoundly changed; carrier diffusion becomes important, but the high-temperature kinetics are not well understood. Now, both the thermal quenching and the thermal red shift are essentially kinetic effects, and the kinetics under low-energy excitation are also not well understood.[28] It is, however, entirely possible that exciting into lower-energy tail states simply reduces the effect of the high temperature on the measured spectrum; this would reduce both the red shift and the quenching. In this case, the small red shift due to lowering the excitation energy may be more than canceled out by the concomitant reduction in the thermal red shift. Such an effect would, of course, only be observable at temperatures sufficiently high that the thermal red shift is larger than the excitation energy red shift; this is consistent with the observations of Bhat *et al.*[14]

This suggestion requires that the thermal quenching will be less drastic when the excitation energy is deep in the tail than under normal, above-gap excitation. The data of Bhat *et al.*[14] does in fact confirm this prediction, for they find that the activation energy of quenching is reduced under low-energy excitation. Thus, the effect of low-energy excitation can be phenomenologically described as a rescaling of the temperature dependence of the PL; although the reason for this is not known (and would depend on the NRR mechanisms), it is sufficient to account for the anomalous blue shift.

D. The kinetics

In the model presented in Sec. III A, it should be possible to derive the kinetics of radiative recombination at low temperature entirely from the competition between the radiative and the thermalization tunneling transitions. A crucial question is then the average separation attained by a geminate pair before radiative recombination, for if this distance is small compared with the average distance between photocreated pairs, then the excitation power will be of no significance and we need only consider the recombination of single pairs. Recombination would be monomolecular and the kinetics would be first order, simplifying the analysis considerably. On the other hand, if geminate pairs separate during thermalization to sufficiently large distances, then carriers from different pairs will recombine with each other, and in the analysis we must consider the complete distant-pair system.[12]

To some extent, this may be considered a problem to be resolved experimentally; however, the evidence is somewhat unclear[49,30] and so a theoretical solution may be of value.

1. Diffusion of photocreated carriers

A simple approach is to consider the distances over which a carrier may tunnel nonradiatively (i.e., in thermalization) for a given radiative lifetime. As may be readily seen from a comparison between the expressions for radiative and nonradiative tunneling [Eq. (1) with the exponential prefactor given by $\tau_0=10^{-8}$ s and $\omega_0=10^{12}$ Hz, respectively, as in Sec. III C 1], for a given transition rate the thermalization transition goes over a distance of $\ln(\omega_0\tau_0)\alpha^{-1}=55$ Å further. Thus even at very short times, in terms of the radiative recombination, a carrier is likely to have made thermalization transitions of the order of 55 Å or longer; this distance corresponds to a radiative lifetime of 0.1 ms. During this time, the carrier is likely to make thermalization transitions of up to 110 Å, equivalent in turn to a radiative lifetime of 1 s, and so on. Thus only the chance of the random walk bringing the carrier back to its geminate partner can result in geminate recombination; more often, a carrier will be closer to another geminate pair and before radiative recombination occurs the carriers can be considered to be distributed at random in space.

An explicit, although approximate, calculation of the distribution of separations of a geminate pair may be carried out. We consider one carrier only, and calculate the random variable given by its distance from the origin during a random walk, the steps of which increase in length as the density of states below the carrier decreases, until radiative recombination intervenes. Thus any correlation between the directions of successive steps is ignored. We use an approximation for the distribution of length of a step; and to keep the calculation simple we do not use a random variable for the decrease in density of states below the carrier. Note that all these approximations *underestimate* the separation of a geminate pair.

The initial distribution of geminate-pair separations, $P_0(r)$, after thermalization to the band edge, is then a δ function $\delta(0,r)$ and the distribution of separations of carriers that recombine at this step, $R_0(r)$, vanishes. If the density of tail states below a carrier before the nth step is ρ_n, then the probability that the nearest is at a distance r is

$$T_n(r)=4\pi r^2\rho_n\exp(-\tfrac{4}{3}\pi r^3\rho_n)\ , \tag{8}$$

and we may take this as the distribution of tunneling distance for the nth step. We convert to one dimension using[50]

$$f(x)=\int_x^\infty r^{-1}F(r)dr\ ,$$

and to make the integral simpler we set $T(r)=4\pi r^2\rho$ for $0\le r\le r_c$ and $T(r)=0$ otherwise. The limiting radius is given by $r_c^3=3/(4\pi\rho)$. Now, if the density of tail states below a carrier before the nth tunneling transition is ρ_n, afterwards it is a random variable distributed evenly over the interval 0 to ρ_n; here we approximate by allowing $\rho_{n+1}=\rho_n/2$. Formation of the convolution of the two distributions $p_n(x)$ and $t_n(x)$ gives $p_{n+1}(x)$, the distribution of x components of the geminate pair separation distribution after the nth transition. To convert back to three dimensions,[50]

$$F(r)=-r\,df(r)/dr\ .$$

The carriers stop tunneling once they have no nearest-neighbor empty defect within a radius r_{cr} such that the radiative time is shorter than the tunneling time; this reduces the probability of tunneling below unity when

$$r_c>r_{cr}\ , \tag{9}$$

and so we take out part of the distribution $P(r)$ after Eq. (9) is satisfied and use r_{cr} in place of r_c in Eq. (7). We then have

$$\begin{aligned} &R_{n+1}(r)=R_n(r)+P_n(r)(1-r_{cr}^3/r_c^3)\ ,\\ &P_n(r)\rightarrow P_n(r)r_{cr}^3/r_c^3\ ,\\ &p_{n+1}(x)=p_n(x)*t_n(x)\ . \end{aligned} \tag{10}$$

The convolution is repeated until the integral over $R(r)$ reaches unity, and so the distribution of geminate pair separations by the time radiative recombination intervenes is given by the limit $R_\infty(r)$. A numerical calculation of $R_\infty(r)$ gives a curve very similar to a three-dimensional (3D) Gaussian in r with a mean of $1.22r_{cr}$ and a standard deviation of one-half (as expected for a 3D Gaussian centered on the origin). Setting $r_{cr}=125$ Å corresponds to a lifetime of 1 ms and radiative recombination over distances ~ 70 Å; the expectation value of R_∞ is about 150 Å. This distance is large compared with the separation over which radiative recombination can occur, thus justifying our assumption that the carriers are distributed at random and recombine with carriers other than their geminate partner.

2. *Kinetics of carriers trapped at random*

From the preceding section, it is clear that at long times we can treat the carriers as distributed at random. If we make the approximation that they thermalize first, are trapped, and only then recombine radiatively, we have the situation described as distant-pair recombination, and treated theoretically in detail by many authors (see Refs. 12, 38, 51, and references therein). The kinetics of distant-pair recombination will therefore be described here only briefly; we then go on to discuss in more detail the experimental results, and the ways in which the situation in *a*-Si:H is in fact more complicated than simple distant-pair recombination.

Distant-pair kinetics are dominated by the exponential in pair separation in Eq. (1). A distribution in pair separation results in a similar distribution in radiative lifetime on a logarithmic scale—that is, a very wide distribution of lifetimes. This leads to decay curves which approximate to power laws; we obtained $I(t)\sim t^{-1}$.[12] As decay proceeds, pairs of short separation recombine, so that at longer times the distribution of pair separations is no longer random. Indeed, after a time corresponding to decay at about 10 Bohr radii ($20\alpha^{-1}$), the PL emission intensity is close to vanishing; however, there remains a density of pairs of the order of one per sphere of radius $20\alpha^{-1}$. These carriers can be termed a metastable excited-state population. They have a profound effect on the kinetics observed by time-resolved spectroscopy (TRS)—at low pulse intensities, the decay curve becomes independent of the pulse intensity.[7] The presence of the metastable population was demonstrated by a comparison of TRS and frequency-resolved spectroscopy (FRS) data[11,12,48] (see also Sec. III D 5).

3. *The metastable excited-state population*

Metastable excited states can be observed in *a*-Si:H by a variety of techniques. Photoluminescence can be observed to as much as 10 s after the pulse;[52] although it is very weak, observable emission from centers with such long lifetimes implies a high density of centers. Light-induced ESR (LESR) provides a direct measurement; good quality *a*-Si:H is diamagnetic in equilibrium and optical excitation produces paramagnetic states with a wide distribution of lifetimes extending up to hours.[53(a),54] Street and Biegelsen[47] concluded from a comparative study of the kinetics of LESR and PL that the LESR centers are the tail-state carriers which give rise to PL; we showed that the LESR centers have distant-pair recombination kinetics.[55] There is, however, no direct proof that the LESR centers can be identified with the PL carriers; for a discussion of this point see Ref. 56.

Less direct ways of observing a metastable population depend on detrapping. Chenevas-Paule and Dijon[57] have observed thermally stimulated currents in diodes minutes or hours after excitation; their spectrum (against temperature) suggests that some originate in tail states.[35] Hoheisel *et al.*[39] reported photoconductivity stimulated by infrared (IR) radiation in previously excited samples. We have obtained similar results with infrared-stimulated photoluminescence.[53(b)]

Thus there is plenty of evidence that excitation at low temperature leads to a significant population of metastable excited carriers. The principal difficulties remaining are to identify the states in which they are trapped, and to establish the density. LESR observes only some 10^{16} cm^{-3}, probably trapped in tail states. TSC observes about the same density, also most likely in tail states. Distant-pair theory predicts some 10^{17} cm^{-3} in the radiative states.[12] Infrared-stimulated luminescence measures close to this density.[53(b)] From IR-stimulated photoconductivity, densities of 10^{19} cm^{-3} have been reported,[39] but we have shown that these values were overestimated by 2 orders of magnitude because of retrapping.[53(b)] Finally, we note that the multiple trapping model (MTM) of dispersive transport[58] would predict that at low temperatures most carriers would be trapped in the tails, and so in this model the metastable populations would be high (they

would, of course, be limited by tunneling recombination to which distant-pair theory would then apply).

4. Calculations of the metastable population

In the preceding section, we have seen that different methods (ESR, photoconductivity, photoluminescence) give similar experimental values for the metastable population density ($\rho_{met} \sim 10^{17}$ cm^{-3}). Meanwhile, theoretical calculations of ρ_{met} were given in Ref. 12; it was assumed that carriers first thermalize and then, once trapped on their final sites, recombine by radiative tunneling. We have seen above that thermalization transitions in the conduction band are faster and go further than the radiative transitions; this implies that the lower part of the tail becomes saturated. If the holes had the same parameter values, a single close, pair of deep tail states could act as a sink for a very large radius around, thus reducing the metastable population. However, the difference in parameters (Table I) prevents this effect and leaves the calculations of Ref. 12 approximately correct. The electrons are able to refill a lower tail state which becomes unoccupied through recombination; the valence-band tail states are not, however, saturated. Consequently, ρ_{met} is primarily determined by the radiative transition rate between deep electron states and occupied hole states, rather than by thermalization transition rates.[12]

5. Frequency response spectroscopy at low temperature

A full analysis of FRS spectra from distant-pair systems is beyond the scope of this paper. Experimental results are shown in Fig. 8, and we wish to show only that they are qualitatively in agreement with the model. FRS is carried out using a continuous pump with a small sinusoidal modulation; luminescence is detected using a lock-in set in quadrature to the modulation. The FRS spectrum is obtained by sweeping the modulation frequency, and is a direct measure of the lifetime distribution

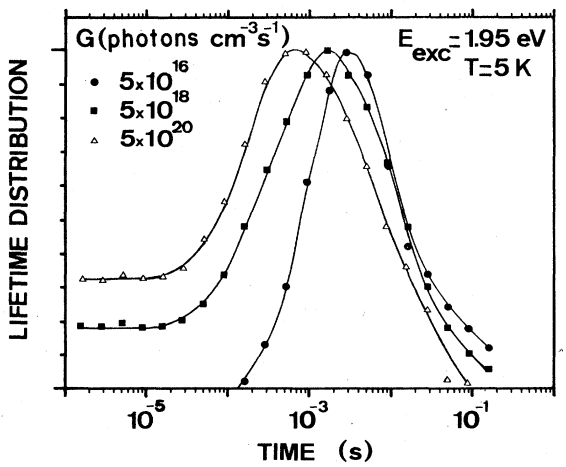

FIG. 8. FRS spectra (lifetime distributions) taken at low temperature and for different excitation rates G. The curves are guides for the eye.

present under continuous excitation.[48] Now, a photoexcited carrier has a probability of $\frac{1}{2}$ of recombining with a carrier already there; these are distributed nearly at random relative to it and this contribution to the lifetime distribution thus depends only on the photoexcited carrier population density. The other one-half of the recombination probability is with carriers created subsequently; it is possible to show that the contribution to the FRS signal of this $\frac{1}{2}$ chance of recombination is identical to the contribution of the first. Thus the FRS spectrum is the lifetime distribution of carriers put into a random distribution of carriers of the density actually present under continuous excitation. At high powers, this density $\rho(G)$ depends quite strongly on pump rate G—in the limit of high G, $\rho \sim G^{1/2}$—while at low power, the density becomes nearly independent of G. This is consistent with the data of Fig. 8, in which the FRS spectrum shifts to lower frequency with reduced power, but the rate of shift is slower at low power.

6. Conclusion

The kinetics of the model of Sec. III A have not been derived rigorously, and further progress would probably require Monte Carlo methods. However, the experimental behavior can be understood at least quantitatively.

IV. OPTICALLY DETECTED MAGNETIC RESONANCE

Optically detected magnetic resonance (ODMR) detects changes in the PL intensity when ESR is performed on paramagnetic centers which are related to the luminescence. ODMR has been reviewed by Cavenett.[59] In crystalline semiconductors this technique has proved to be valuable for identifying recombination centers, deconvolving unresolved emission bands, and for studies of the kinetics of recombination.[60,61] ODMR has been studied in a-Si:H since 1978, but there has been little agreement on the experimental results, their interpretation, or on the recombination mechanisms involved.[5,56,62,63]

In intrinsic samples, ESR detects a single signal at $g=2.0055$ attributed to dangling bonds,[64] while under optical excitation two further resonances are observed at $g=2.004$ and 2.013 (with half widths of 5 and 25 G, respectively). These LESR resonances are thought to be due to carriers trapped in conduction- and valence-band tail states.[47] Both the basic models of the high-energy PL band of Secs. II and III assume that the radiative states are the band tail states; and since radiative recombination is subject to spin selection rules, in the distant-pair model an enhancing ODMR signal consisting of the sum of the LESR resonances is expected. However, in different samples, the ODMR enhancing resonance is either a 19-G-wide line at $g=2.0078$, or a 200-G line at $g \cong 2.01$, or a superposition of the two,[56] and this result would seem to suggest that the LESR states are not the radiative states for PL. Other authors have indeed suggested that centers such as the dangling bond[65] or the A center[66] are associated with the 1.4-eV PL band.

We have recently shown that the LESR signals are suf-

ficient to account for the ODMR enhancing signal, and therefore it is not necessary to invoke centers other than the tail states to account for the PL.[56] In agreement with ideas suggested by Depinna *et al.*[62] and Street,[63] we found that time-resolved ODMR signals were consistent with exchange interaction between the recombining carriers. This mixes the tail-state resonances, either into a single line at the average g value (this accounts for the $g=2.0078$ line) when spin-allowed transitions are dominant, or into a broad line when the transitions are spin forbidden (triplet singlet). PL is proportional to the radiative recombination rate, while LESR is sensitive to the number of carriers; consequently, ODMR is more sensitive to short-lived carriers with a stronger exchange interaction, while LESR strongly weights the contribution from more distant pairs with a weaker exchange interaction. On this basis, we have shown that the ODMR results are fully consistent with the model in which both LESR and PL are due to distant-pair tail-state carriers as in the model of Sec. III.[56]

Some characteristics of the kinetics of the 1.4-eV PL were also inferred from ODMR. The observation of a quenching ODMR signal and its similarity to the LESR signal was taken as evidence for geminate recombination.[10] If electron-hole pairs are geminate, and if spin relaxation is not complete, there will be a preponderance of pairs in the singlet spin state. Resonance of either carrier will then increase the triplet population; since radiative recombination of triplet pairs is spin forbidden, the PL will decrease in intensity. This model has also been used recently by Homewood *et al.*[67] to account for an enhancing signal seen in pin diodes by photovoltaic detected magnetic resonance (PDMR). However, the waveform of the response of the PL intensity to the microwave modulation at resonance can give considerable information on the details of the spin-dependent process,[60] and Depinna *et al.*[62] were thereby able to show that the quenching signal is due to an enhancing resonance in a shunt (competing) process. It is possible that the PDMR results[67] may also be explained by spin-dependent mobility effects in the doped layers of the pin diode. Such effects have recently been measured in the dark conductivity of doped a-Si:H.[68] The quenching ODMR signal is similar to quenching signals observed in spin-dependent photoconductivity,[69] spin-dependent photoinduced absorption,[70] and PDMR.[67] All these signals are likely to be different aspects of the same spin-dependent recombination mechanism reducing the lifetime of the tail-state carriers. The dangling bond is usually considered to be the dominant nonradiative recombination center, and Boulitrop has shown that its charge state is an important parameter.[56]

In conclusion, we think that ODMR data is consistent with, and generally supports, the model for the radiative recombination of Sec. III.

V. CONCLUSIONS

The model presented in this paper provides a satisfactory understanding of all aspects of the high-energy photoluminescence of a-Si:H that are *unrelated* to nonradiative recombination. A good understanding of a fundamental process such as intrinsic radiative recombination might be expected to be very helpful in understanding the electronic structure of the semiconductor. Regrettably, in the case of a-Si:H, this is not so. Had there been detailed structure in the PL, a great deal of information on the electronic structure could undoubtedly have been extracted; if some of the earlier models discussed in Sec. II had turned out to be correct, again, information on the electronic structure would have been implicit. However, our model is the simplest model consistent with the known properties of a-Si:H; that it turns out to be consistent with the experimental behavior of the PL means that no new information is contained in the PL data. It cannot even be claimed that this result provides support for the tail-state picture within which our model is here expressed, for the model starts with few, and general, assumptions that may also be fulfilled by other fundamental pictures. Indeed, our model was originally derived from the band-gap fluctuation model of amorphous semiconductors[22] and is also consistent with that picture.[13]

This may appear to be a pessimistic conclusion. On a more positive note, it is encouraging that the PL can be explained so simply. Thorough analysis of the simple model leads to many counterintuitive results; this may prompt speculation that some of the unexplained phenomena in amorphous semiconductors (such as the Meyer-Neldel rule,[71] or the Urbach tails[72]) will also yield to proper analysis of a simple model. Furthermore, the model presented here for a-Si:H makes no appeal to any properties peculiar to a-Si:H. It is therefore likely that it is directly applicable to the photoluminescence of other amorphous systems.[13]

ACKNOWLEDGMENTS

We wish to thank the Centre d'Etudes Nucléaires de Grenoble and Linz University where some of this work has been carried out and Professor I. Solomon for helpful discussions.

[1]R. A. Street, Adv. Phys. **30**, 593 (1980).
[2]R. A. Street, Philos. Mag. B **37**, 35 (1978).
[3]S. Griep and L. Ley, J. Non-Cryst. Solids **59&60**, 253 (1983).
[4]"It is vain to do with more what can be done with fewer"—William of Ockham, *Summa Logicae* (Paris, 1488).
[5]D. Engemann and R. Fischer, Phys. Status Solidi B **79**, 195 (1977).
[6]K. Morigaki, D. J. Dunstan, B. C. Cavenett, P. Dawson, J. E. Nicholls, S. Nitta, and K. Shimakawa, Solid State Commun. **26**, 981 (1978).
[7]C. Tsang and R. A. Street, Phys. Rev. B **19**, 3027 (1979).
[8]T. M. Searle, T. S. Nashashibi, I. G. Austin, R. Devonshire, and G. Lockwood, Philos. Mag. B **39**, 389 (1979).
[9]W. B. Jackson and R. J. Nemanich, J. Non-Cryst. Solids

59& 60, 353 (1983).
[10]D. K. Biegelsen, J. C. Knights, R. A. Street, C. Tsang, and R. M. White, Philos. Mag. B **37**, 477 (1978).
[11]D. J. Dunstan, S. P. Depinna, and B. C. Cavenett, J. Phys. C **15**, L425 (1982).
[12]D. J. Dunstan, Philos. Mag. B **46**, 579 (1982).
[13]F. Boulitrop and D. J. Dunstan, Phys. Rev. B **28**, 5923 (1983).
[14]P. K. Bhat, T. M. Searle, I. G. Austin, R. A. Gibson, and J. Allison, Solid State Commun. **45**, 481 (1983).
[15]R. A. Street, Solid State Commun. **34**, 157 (1980).
[16]R. W. Collins and W. Paul, J. Phys. (Paris) Colloq. **42**, C4-591 (1981).
[17]B. A. Wilson, P. Hu, J. P. Harbison, and T. M. Jedju, J. Non-Cryst. Solids **59& 60**, 341 (1983).
[18]W.-C. Chen, B. J. Feldman, J. Bajaj, F.-M. Tong, and G. K. Wong, Solid State Commun. **38**, 357 (1981).
[19]R. W. Collins, M. A. Paesler, G. Moddell, and W. Paul, J. Non-Cryst. Solids **35/36**, 681 (1980).
[20]J. I. Pankove, F. H. Pollak, and C. Schnabolk, J. Non-Cryst. Solids **35/36**, 459 (1980).
[21]R. W. Collins and W. Paul, Phys. Rev. B **25**, 2611 (1982).
[22]D. J. Dunstan, Solid State Commun. **43**, 341 (1982).
[23]T. M. Searle, Philos. Mag. B **46**, 163 (1982).
[24]R. A. Street, J. C. Knights, and D. K. Biegelsen, Phys. Rev. B **18**, 1880 (1978).
[25]R. W. Collins, P. Viktorovitch, R. L. Weisfeld, and W. Paul, Phys. Rev. B **26**, 6643 (1982).
[26]D. J. Dunstan, Philos. Mag. B **49**, 191 (1984).
[27]R. A. Street, Phys. Rev. B **23**, 861 (1981).
[28]P. K. Bhat, D. J. Dunstan, I. G. Austin, and T. M. Searle, J. Non-Cryst. Solids **59& 60**, 349 (1983).
[29]D. R. Wake and N. M. Amer, Phys. Rev. B **27**, 2598 (1983).
[30]D. J. Dunstan, Solid State Commun. **49**, 395 (1984).
[31]F. Boulitrop, D. J. Dunstan, and A. Chenevas-Paule, Phys. Rev. B **25**, 7860 (1982).
[32]E. Merk, W. Czaja, and K. Maschke, Helv. Phys. Acta **56**, 896 (1983).
[33]N. F. Mott and E. A. Davis, *Electronic Processes in Non-Crystalline Materials* (Clarendon, Oxford, 1979).
[34]T. Tiedje, A. Rose, and J. M. Cebulka, *Tetrahedrally Bonded Amorphous Semiconductors (Carefree, Arizona),* Topical Conference on Tetrahedrally Bonded Amorphous Semiconductors, edited by R. A. Street, D. K. Biegelsen, and J. C. Knights (AIP, New York, 1981), p. 197.
[35]J. Dijon, Solid State Commun. **48**, 79 (1984).
[36]M. Stutzmann and J. Stuke, Solid State Commun. **47**, 1635 (1983).
[37]D. Redfield, Solid State Commun. **44**, 1347 (1982).
[38]W. Hoogenstraaten, Philips Res. Rep. **13**, 515 (1958).
[39]M. Hoheisel, R. Carius, and W. Fuhs, J. Non-Cryst. Solids **59& 60**, 457 (1983).
[40]J. Tauc, Festkörperprobleme **22**, 85 (1982).
[41]D. J. Dunstan and F. Boulitrop, J. Phys. (Paris) Colloq. **42**, C4-331 (1981).
[42]D. J. Dunstan, Phys. Rev. B **28**, 2252 (1983).
[43]L. Onsager, Phys. Rev. **54**, 554 (1938).
[44]J. Noolandi, K. M. Hong, and R. A. Street, Solid State Commun. **34**, 45 (1980).
[45]H. Fritzche, J. Non-Cryst. Solids **6**, 49 (1971).
[46]J. Tauc, Mater. Res. Bull. **5**, 721 (1970).
[47]R. A. Street and D. K. Biegelsen, Solid State Commun. **33**, 1159 (1980).
[48]S. P. Depinna and D. J. Dunstan, Philos. Mag. B (to be published).
[49]R. A. Street and D. K. Biegelsen, Solid State Commun. **44**, 501 (1982).
[50]See, e.g., W. Feller, *An Introduction to Probability Theory and its Applications* (Wiley, London, 1966), Vol. II, Chap. I.10.
[51]D. G. Thomas, J. J. Hopfield, and W. M. Augustyniak, Phys. Rev. **140**, A202 (1965).
[52]F. Boulitrop, thesis, Université Scientifique et médicale Grenoble, 1982.
[53](a) F. Boulitrop, J. Dijon, D. J. Dunstan, and A. Hervé, in *International Conference on the Physics of Semiconductors, San Francisco* (in press); (b) F. Boulitrop, in *Conference on Optical Effects in Amorphous Semiconductors, Salt Lake City* (in press).
[54]A. Friederich and D. Kaplan, J. Elect. Mater. **8**, 79 (1979).
[55]F. Boulitrop and D. J. Dunstan, Solid State Commun. **44**, 841 (1982).
[56]F. Boulitrop, Phys. Rev. B **28**, 6192 (1983).
[57]A. Chenevas-Paule and J. Dijon, J. Phys. (Paris) Colloq. **42**, C4-605 (1981).
[58]H. Scher and E. W. Montroll, Phys. Rev. B **12**, 2455 (1975).
[59]B. C. Cavenett, Adv. Phys. **30**, 475 (1981).
[60]D. J. Dunstan and J. J. Davies, J. Phys. C **12**, 2927 (1979).
[61]D. Block, A. Hervé, and R. Cox, Phys. Rev. B **25**, 6049 (1982).
[62](a) S. P. Depinna, B. C. Cavenett, T. M. Searle, and I. G. Austin, Philos. Mag. B **46**, 501 (1982); (b) S. P. Depinna, Phys. Rev. B **28**, 5327 (1983).
[63]R. A. Street, Phys. Rev. B **26**, 3588 (1982).
[64]M. H. Brodsky and R. S. Title, Phys. Rev. Lett. **23**, 581 (1969).
[65]S. P. Depinna, B. C. Cavenett, I. G. Austin, and T. M. Searle, Solid State Commun. **41**, 263 (1982).
[66]K. Morigaki, P. Dawson, B. C. Cavenett, D. J. Dunstan, S. Nitta, and K. Shimakawa, in *Proceedings of the 14th Conference on Amorphous and Liquid Semiconductors, Edinburgh, 1978,* edited by B. C. H. Wilson (IOP, Bristol, 1979), p. 1163.
[67]K. P. Homewood, B. C. Cavenett, W. E. Spear, and P. G. LeComber, J. Phys. C **16**, L427 (1983).
[68]U. Dersch, H. Muller, B. Pohlmann, and P. Thomas, J. Non-Cryst. Solids **59& 60**, 61 (1983).
[69]I. Solomon, D. K. Biegelsen, and J. C. Knights, Solid State Commun. **22**, 505 (1977).
[70]I. Hirabayashi and K. Morigaki, J. Non-Cryst. Solids **59& 60**, 133 (1983).
[71]P. Irsigler, D. Wagner, and D. J. Dunstan, J. Phys. C **16**, 6605 (1983).
[72]D. J. Dunstan, J. Phys. C **15**, L419 (1982).